pubs.acs.org/Biomac

Article

Heparinized Gelatin-Based Hydrogels for Differentiation of Induced Pluripotent Stem Cells

Matthew R. Arkenberg, Karl Koehler, and Chien-Chi Lin*

Cite This: *Biomacromolecules* 2022, 23, 4141−4152

Read Online

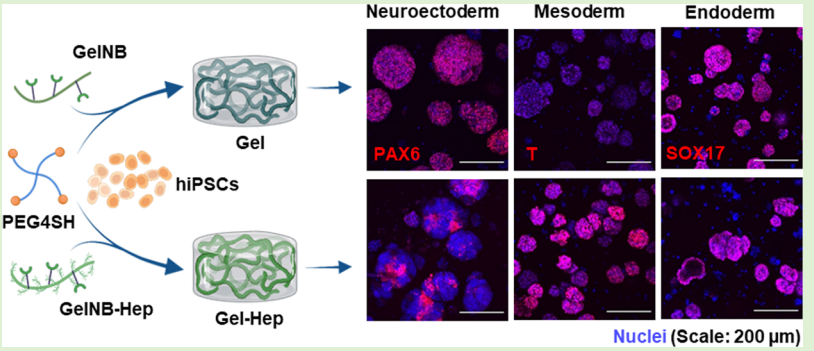

ABSTRACT: Chemically defined hydrogels are increasingly utilized to define the effects of extracellular matrix (ECM) components on cellular fate determination of human embryonic and induced pluripotent stem cell (hESC and hiPSCs). In particular, hydrogels cross-linked by orthogonal click chemistry, including thiol-norbornene photopolymerization and inverse electron demand Diels−Alder (iEDDA) reactions, are explored for 3D culture of hESC/hiPSCs owing to the specificity, efficiency, cytocompatibility, and modularity of the cross-linking reactions. In this work, we exploited the modularity of thiol-norbornene photopolymerization to create a biomimetic hydrogel platform for 3D culture and differentiation of hiPSCs. A cell-adhesive, protease-labile, and cross-linkable gelatin derivative, gelatin-norbornene (GelNB), was used as the backbone polymer for constructing hiPSC-laden biomimetic hydrogels. GelNB was further heparinized via the iEDDA click reaction using tetrazine-modified heparin (HepTz), creating GelNB-Hep. GelNB or GelNB-Hep was modularly cross-linked with either inert macromer poly(ethylene glycol)-tetra-thiol (PEG4SH) or another bioactive macromer-thiolated hyaluronic acid (THA). The formulations of these hydrogels were modularly tuned to afford biomimetic matrices with similar elastic moduli but varying bioactive components, enabling the understanding of each bioactive component on supporting hiPSC growth and ectodermal, mesodermal, and endodermal fate commitment under identical soluble differentiation cues.

1. INTRODUCTION

Human pluripotent stem cells (hPSCs), including embryonic and induced pluripotent stem cells (hESCs and hiPSCs), are invaluable for regenerative therapies, toxicology screening, disease modeling, and basic research in developmental biology.[1] The PSC fate determinate (e.g., quiescence, self-renewal, differentiation) is guided by a plethora of soluble and immobilized biophysical−chemical cues of the extracellular matrix (ECM),[2] with which to facilitate the understanding and recapitulation of the stem cell niche. For example, animal-derived basement membrane (BM) extracts (e.g., Matrigel, Geltrex) have been used in various studies to generate PSC-derived organoids.[3] However, the batch-to-batch variability and ill-defined compositions of BM extracts pose significant challenges for basic research and clinical translation of PSC differentiation and organoid generation. To this end, hydrogels consisting of synthetic materials (e.g., poly(ethylene) glycol, PEG) and naturally derived macromolecules (e.g., gelatin, heparin, hyaluronic acid) are increasingly being developed for PSC culture and differentiation. For example, 4-arm PEG-maleimide hydrogels cross-linked by protease labile peptides were used to support the maturation of human intestinal organoids.[4] However, in this study, the initial expansion of PSC-derived intestinal stem cells was still conducted in Matrigel. It was not clear whether chemically defined hydrogels could be employed for *in situ* generation of embryoid body prior to their lineage specific differentiation of iPSCs.

Ideally, engineered matrices should facilitate self-renewal and expansion of PSC populations[5,6] while also supporting lineage-

Received: May 9, 2022
Revised: August 11, 2022
Published: September 8, 2022

https://doi.org/10.1021/acs.biomac.2c00585
Biomacromolecules 2022, 23, 4141−4152

specific differentiation.[7−10] For example, Ekerdt and colleagues developed a thermo-reversible hyaluronic acid-poly(*N*-isopropylacrylamide) (HA/PNIPAAm) hydrogel to support long-term survival and self-renewal of hPSCs.[5] In another example, Nazari *et al.* showed that the use of fibrin hydrogels significantly increased differentiation of hiPSCs into oligodendrocytes as compared with a two-dimensional (2D) culture.[10] As major ECM components, heparin and HA have both been used to support *in vitro* culture and differentiation of PSCs.[9,11−15] Heparin is capable of sequestering and stabilizing numerous growth factors, such as the basic fibroblast growth factor (bFGF) and transforming growth factor beta-1 (TGF-β1),[16−18] both of which maintain pluripotency and viability of PSCs.[19] In addition, heparin has been shown to regulate mesoderm and ectoderm differentiation of PSCs by modulating the Wnt signaling pathway. In particular, heparin induced inhibition of glycogen synthase kinase-3β (GSK-3β) and stabilized β-catenin during neuronal morphogenesis.[11] With respect to mesoderm commitment, addition of soluble heparin enhanced brachyury (T) and Wnt3A expression.[12] However, heparin may inhibit Axin2, a molecule downstream of Wnt signaling, which promotes cardiomyocyte development.

Compared with soluble heparin, immobilization of heparin in hydrogels may offer several benefits, including sustained signaling, growth factor sequestration and stabilization, and reduced growth factor dosing owing to the need for daily media exchanges in a PSC culture.[9] Immobilization of heparin in hydrogels can be achieved using a variety of bioconjugation chemistry, including standard carbodiimide chemistry,[20,21] Michael-type addition between thiol and maleimide functional groups[22] or between thiol and acrylate groups,[23] thiol-norbornene photoclick reaction, and inverse electron demand Diels−Alder (iEDDA) tetrazine-norbornene reaction.[7,24] For example, Brown and colleagues utilized methacrylated- or thiolated-heparin along with gelatin-methacryloyl (GelMA) to enhance chondrocyte viability and matrix deposition.[25] Siltanen *et al.* utilized heparin-methacrylate for its immobilization/cross-linking with 8-arm PEG-thiol (PEG8SH) and PEG-diacrylate (PEGDA) into microgels via Michael addition.[9] The heparin-immobilized microgels were found to enhance expression of definitive endoderm (DE) markers in mouse ESCs (mESCs).

HA has been implicated in embryogenesis[26] and hESC growth/differentiation *in vivo*.[27] Gerecht and colleagues first described the use of methacrylated-HA hydrogels for encapsulation and maintenance of pluripotency of hESCs.[13] More recently, Miura and colleagues demonstrated that highly sulfated HA was capable of maintaining hiPSCs in an undifferentiated state under feeder-free and bFGF-free conditions.[14] Both HA and heparin synergistically enhanced development of PSC-derived brain organoids.[15] Specifically, soluble heparin and HA supported ectoderm differentiation, and photo-cross-linked heparin-HA hydrogels directed neural patterning toward a hindbrain fate.[15] Nonetheless, the effect of immobilized heparin and HA on fate trilineage fate commitment of iPSCs *in vitro* remains understudied.

In this study, we sought to evaluate the potential of engineered hydrogels for *in situ* proliferation and trilineage differentiation of iPSCs. We explored gelatin, heparin, and HA as the bioactive building blocks for fabricating hydrogels via thiol-norbornene and tetrazine-norbornene click chemistries. Specifically, norbornene-functionalized gelatin (GelNB) served as the backbone of the cross-linked hydrogels. While proteolytically labile and cell adhesive gelatin has been widely used as a substrate for the 2D cell culture,[28−30] its use for the 3D culture of hiPSCs is limited. Via thiol-norbornene photocross-linking, GelNB was used to cross-link thiolated cross-linkers, including multi-arm PEG-thiol (e.g., PEG-tetra-thiol or PEG4SH) or thiolated HA (THA).[31] When NB moieties are in excess, GelNB may be further functionalized with tetrazine-containing molecules (i.e., heparin-tetrazine, HepTz) via the iEDDA click reaction owing to its dual reactivity toward thiol and tetrazine. A number of macromolecules have been functionalized with tetrazine moieties including gelatin,[32] PEG,[33] and heparin.[24] To develop modular polysaccharide nanoparticles, our lab generated HepTz to afford electrostatic complexation between heparin and poly(L-lysine), where the Tz moiety was used for further functionalization of the particles.[24] Given the previous literature supporting the modulation of critical PSC signaling pathways in the presence of heparin and HA, we investigated the effects of these 3D hydrogels on hiPSC pluripotency and trilineage commitment of hiPSCs.

2. MATERIALS AND METHODS

2.1. Materials. Type A Gelatin (238−282 Bloom) was purchased from Amresco. Carbic anhydride and 1-(3-dimethylaminopropyl)-3-ethylcarbodiimide hydrochloride (EDC) were purchased from Acros. *N*-hydroxysuccinimide was purchased from TCI. Four-arm PEG-SH (PEG4SH, 10 kDa) was obtained from Laysan Bio. Heparin sodium salt was obtained from Celsus Laboratories, and THA (~300 kDa) was purchased from ESI Bio. Tetrazine-amine (Tz-NH_2) was obtained from Click Chemistry Tools. Type 1 Collagenase and hyaluronidase were obtained from Worthington. Lithium aryl phosphinate (LAP) and L-ascorbic acid were obtained from Sigma Aldrich. All other chemicals were purchased from Fisher Scientific unless noted otherwise.

2.2. Synthesis of Macromers. Macromer Type A GelNB was synthesized as described previously without modification.[34] Substitution of NB (~3.5 mM NB/wt% Gel) was confirmed by the fluoraldehyde assay. Low substitution HepTz was synthesized as described previously using carbodiimide coupling chemistry.[24] In a round bottom flask, heparin sodium salt (~500 mg, 16.7 kDa), EDC (2.5× to COOH groups), and NHS (2.5× to COOH groups) were dissolved in 15 mL of ddH_2O. Activation of the carboxylic acid groups proceeded for 30 min prior to adding Tz-NH_2 to the flask. The reaction was proceeded for ~16 h at room temperature protected from light. The product was dialyzed against ddH_2O protected from light for 3 days, lyophilized, and stored at −20 °C until ready to use. The Tz substitution was quantified by measuring characteristic absorbance at 523 nm and comparing against a Tz-NH_2 standard. Heparinization of gelatin was achieved using the tetrazine-norbornene iEDDA reaction. In brief, HepTz was added to Gel-NB at specified concentrations, placed at 37 °C. Consumption of Tz was monitored by periodic measurement of the characteristic peak at 523 nm.

2.3. Mechanical Characterization of Hydrogels. Hydrogels were fabricated under aseptic conditions using thiol-norbornene photopolymerization. Macromer GelNB was mixed with cross-linker PEG4SH or THA at specified concentrations and mixed with photoinitiator LAP (2 mM). After homogenization, the precursor solution was transferred between 1 mm Teflon spacer-separated glass slides. The hydrogels were then subjected to UV-light (365 nm, 5 mW/cm^2) treatment for 2 min to achieve cross-linking. For heparinization of gelatin-based hydrogels, macromers GelNB and HepTz were mixed for ~24 h prior to adding remaining precursor materials and performing gelation as described above. All gels were swollen in sterile DPBS at 37 °C overnight. Unless otherwise specified, formulations utilized for all experiments are given in Table S2. Oscillatory rheometry in strain sweep mode (Bohlin CV100) was utilized to obtain elastic moduli (G'). Dimethylmethylene blue (DMMB) was used to confirm heparin functionalization of the hydrogels. In brief, hydrogels were fabricated as described above, swollen for 16 h at 37 °C, and washed thrice with DPBS (30 min per wash) to remove unreacted HepTz. After washing,

https://doi.org/10.1021/acs.biomac.2c00585
Biomacromolecules 2022, 23, 4141−4152

the gels were incubated in DMMB solution overnight at 37 °C followed by three additional 30 min washes to remove excess DMMB.

2.4. Enzymatic Degradation of Hydrogels. For collagenase degradation measurements, hydrogels were fabricated as specified. After 16 h, the initial mass of the hydrogels was obtained (m_i). The gels were treated with 50 U/mL of type 1 collagenase and weighed periodically (m_t). For hyaluronidase degradation studies, the initial mass was obtained as described above. Following this, gels were subjected to 2000 U/mL hyaluronidase treatment and weighed periodically. The mass remaining is presented as % mass remaining = $100 \times (m_t - m_i)/m_i$. To obtain the mass swelling ratio, hydrogels were formed and swollen in PBS overnight at 37 °C. The hydrogels were weighted to obtain $m_{swollen}$. The gels were dried in vacuo for 24 h and weighed to obtain m_{dried}. The swelling ratio was determined with the following equation: $q = m_{swollen}/m_{dried}$.

2.5. Maintenance and Encapsulation of iPSCs in Gelatin-Based Thiol-Norbornene Hydrogels. Cellartis hiPSC12 cell lines (ChiPSC12, Takara) were cultured on vitronectin coated plates in Essential 8 (E8, Gibco) medium. Vitronectin coating was conducted as per the manufacturer's protocol. For the first 24 h of culture after thawing or passaging, media was supplemented with ROCK inhibitor Y-27632 (E8Y, 10 μM). Media was refreshed daily with cell passaging every 3 to 4 days. Passaging was conducted by washing the cells with DPBS, treating with TrypLE Select dissociation reagent (Gibco) for 5 min.

For encapsulation, dissociated iPSCs were mixed with a pre-polymer solution at specified concentrations to achieve a final density of 2 million cells/mL. After pipetting gently to mix, the cell and precursor mixture was pipetted into a cylindrical mold and treated with UV-light for 2 min to polymerize. For experiments involving Gel-Hep, the GelNB and HepTz precursor components were mixed and incubated for 24 h at 37 °C. The Gel-Hep conjugate was mixed with other pre-polymer components prior to adding the cell suspension and polymerizing as described above. E8Y was changed on D2 post-encapsulation and then daily on D4 and after. Following encapsulation, the cell morphology was monitored via Brightfield imaging and the viability was determined as described previously.[7] Cell proliferation was assessed by adding 10 μM of EdU reagent (Click-IT EdU staining kit) to the culture media on D3 post-encapsulation. Incubation with EdU was conducted for 24 h followed by washing the cell laden gels with DPBS twice and gel fixation with 4% paraformaldehyde. The gels were permeabilized with 0.5% Triton X-100 for 30 min followed by washing with DPBS 2× and treatment with EdU reaction cocktail prepared via the manufacturer's protocol. The gels were counterstained with DAPI for 1 h and washed twice with DPBS prior to imaging. All imaging was conducted using a confocal microscope (Olympus Fluoview FV100 laser scanning microscope). At least three regions of interest were imaged per sample (10 slices, 10 μm per slice).

2.6. Trilineage Differentiation of Encapsulated iPSCs. To induce mesoderm cell differentiation of encapsulated ChiPSC12 hiPSCs, E8Y media was replaced with LaSR media (Advanced DMEM/F12, Thermo Fisher Scientific, and ascorbic acid, 60 μg/mL) supplemented with CHIR99021 (6 μM) on D4 post-encapsulation. The differentiating cells were treated with LaSR +CHIR99021 for 2 days in total.[35] Definitive endoderm differentiation was conducted using a STEMdiff Definitive Endoderm Kit (STEMCELL Technologies) on D4 post-encapsulation as per the manufacturer's protocol for 3 days in total. Non-neural ectoderm differentiation was conducted by treating D4 encapsulated iPSCs for four additional days with chemically defined media (CDM) with non-neural ectoderm differentiation supplements as described previously.[36] Neuroectoderm differentiation was conducted using a STEMdiff SMADi neural induction kit (STEMCELL Technologies) on D4 post encapsulation. Cells were treated with NE differentiation media for 7 additional days prior to assessment. Cells were assayed using immunostaining, flow cytometry, and quantitative real-time PCR (qPCR).

2.7. Immunostaining and Imaging of Encapsulated iPSCs. Hydrogels were collected at specified time points and washed at room temperature with DPBS for 5 min. The washed hydrogels were fixed with paraformaldehyde (4%) for 45 min at room temperature. Following one wash with DPBS and two washes with DPBS with 1% bovine serum albumin (BSA) and 0.3% Triton X-100 at 5 min each, the gels were blocked and permeabilized with DPBS containing 1% BSA and 0.3% Triton X-100. After blocking and permeabilization, the hydrogels were incubated overnight at 4 °C with specified primary antibodies (for neuroectoderm: 1:200 diluted rabbit anti-PAX6, Cell Signaling; for non-neural ectoderm: 1:50 diluted mouse anti-AFP2α, Santa Cruz Biotechnology; for mesoderm: 1:200 diluted rabbit anti-T, Cell Signaling; for definitive endoderm: 1:200 diluted rabbit anti-SOX17, Cell Signaling). After three additional washes with DPBS containing 1% BSA and 0.3% Triton X-100 for 45 min each at room temperature, the gels were incubated with corresponding secondary antibodies (1:200 diluted goat anti-mouse AF647, Santa Cruz Biotechnology or 1:200 anti-rabbit AF555, Cell Signaling) overnight at 4 °C. Three additional 30 min DPBS washes were conducted followed by 1 h counterstaining with DAPI nuclear stain. After three final 10 min washes with DPBS, the gels were imaged as described above.

2.8. RNA Extraction, RT-PCR, and TaqMan Array Analysis of iPSCs in 2D and 3D Formats. After 4 days culture in hydrogels or in 2D format, three cell-laden Gel, Gel-HA, Gel-Hep, or Geltrex hydrogels were pooled and incubated with Type 1 collagenase (50 U/mL) for 1 h or until complete degradation. Geltrex hydrogels were pipetted vigorously to disrupt the matrix. 2D samples were dissociated with TrypLE Select as described above. After collection of all samples in DNase/RNase free microtubes, the samples were flash frozen in liquid nitrogen and stored at −80 °C until ready for analysis. RNA extraction was conducted using the NucleoSpin RNA II kit (Clontech) without modification to the manufacturer's protocol. The concentration and quality of RNA was assessed using a NanoDrop 2000 spectrophotometer (Thermo Scientific). A PrimeScript RT reagent kit (Clontech) was utilized to convert the RNA into single-stranded cDNA. A 96-well TaqMan array (Thermo Fisher Scientific) was utilized to assess expression patterning of iPSCs in 2D and 3D formats as described previously. In brief, 10 μL of an equal volume dilution of 100 ng/mL of cDNA and a TaqMan fast universal mix was added to each of the 96 wells. After sealing and vortexing the plate, a QuantStudio 3 Real-Time PCR system was used to collect quantitative PCR (qPCR) data. A total of three biological replicates were used for each condition. The relative fold change to the 2D sample (RQ) was determined with global normalization using DataAssist Software v3.01 (Thermo Fisher). The heat map plot and hierarchical clustering of 63 detected genes ($C_t < 40$) was visualized in DataAssist using Pearson's correlation as the distance measure and average linkage as the clustering method. Volcano plots were generated with a p-value boundary set to <0.05 and a fold change boundary of 2 using Student's t test with a Benjamini−Hochberg false discovery rate procedure conducted. For differentiation studies, an SYBR Premix Ex TAqII kit (Clontech) was used with primers listed in Table S1. 18S was used as the housekeeping gene, and expression was compared against control group Geltrex using the 2^{-ddCt} method.

2.9. Flow Cytometry of Differentiated iPSCs in Gelatin-Based Thiol-Norbornene Hydrogels. Three cell-laden hydrogels from each condition were pooled into a single well. The cells were liberated from the gelatin and heparinized-gelatin hydrogels through 2 h collagenase treatment (50 U/mL). Cells were liberated from Geltrex via vigorous pipetting. The cells were centrifuged (1000 rpm for 3 min) and resuspended in a TrypLE Select dissociation reagent. After 10 min incubation at 37 °C to dissociate the cells clusters, one additional wash with DPBS was conducted. The cells were fixed with 4% PFA for 10 min at room temperature. The cells were washed once with DPBS and blocked/permeabilized with DPBS containing 1% BSA and 0.3% Triton X-100. The cells were incubated with the primary antibodies as describe above at 4 °C overnight. The cells were washed twice with DPBS with 1% BSA and 0.3% Triton X-100 and treated with anti-rabbit AF555 (1:200 dilution) or AF488 (1:200 dilution) for 90 min. After three additional DPBS washes and cell straining, flow cytometry was conducted on a BD LSR II or Fortessa analyzer, and data was analyzed with FlowJo software.

https://doi.org/10.1021/acs.biomac.2c00585
Biomacromolecules 2022, 23, 4141−4152

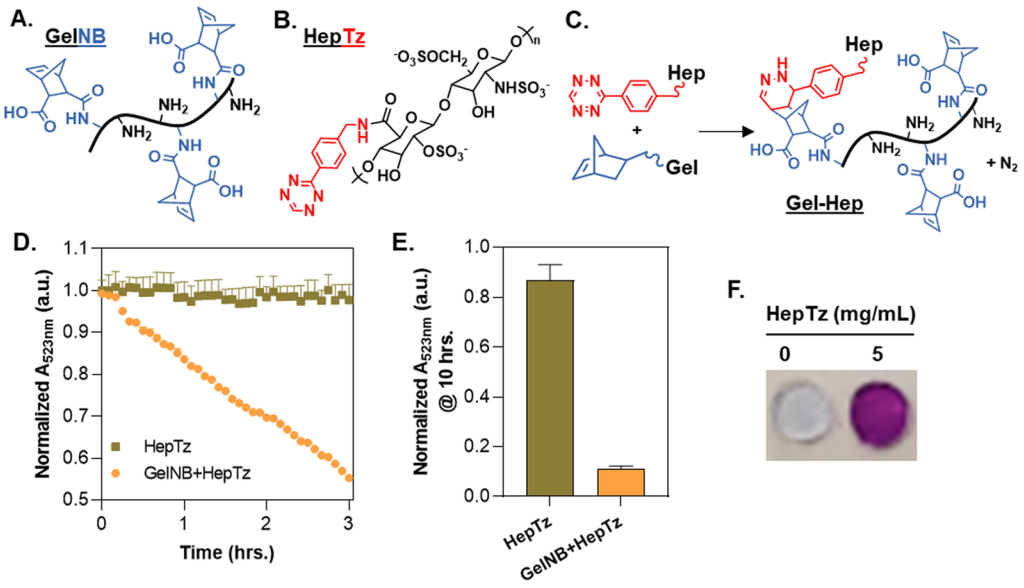

Figure 1. Schematic illustration of (A) GelNB and (B) HepTz. (C) Reaction schematic of the tetrazine-norbornene iEDDA click reaction. (D) Normalized absorbance at 523 nm (A_{523nm}) representing Tz consumption with 0.5 wt % HepTz alone or 0.5 wt % HepTz with 5 wt % GelNB. The reaction was monitored for 3 h. (E) Normalized A_{523nm} of HepTz/GelNB+HepTz after 10 h of iEDDA click reaction. (F) Representative image of DMMB staining of hydrogels containing 0 or 5 mg/mL of HepTz.

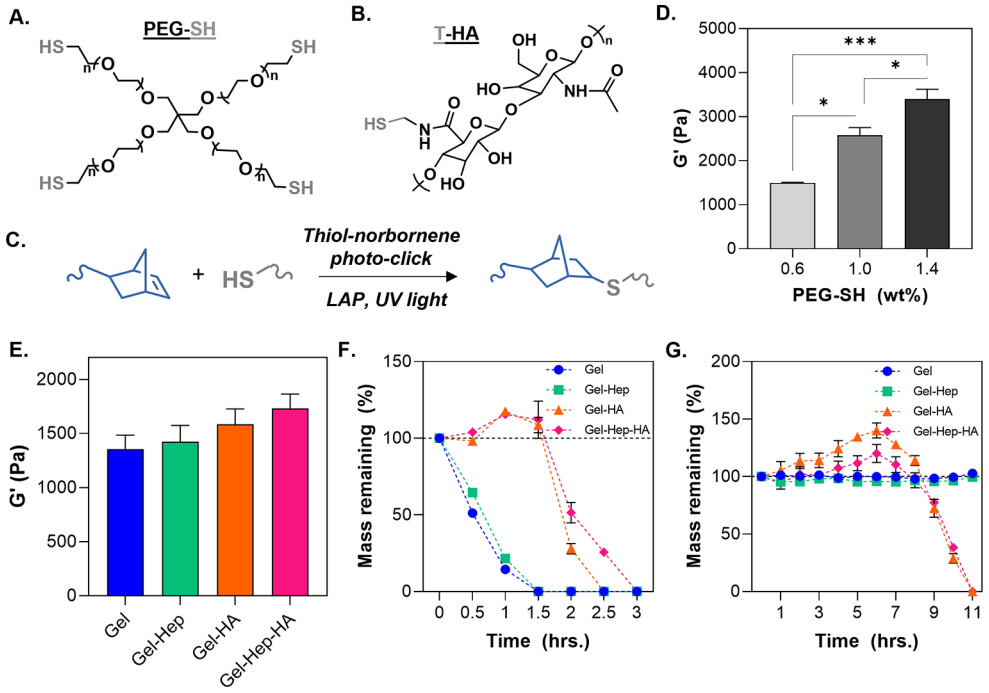

Figure 2. Schematic representation of multifunctional thiol linkers: (A) PEG4SH and (B) THA. (C) Thiol-ene photopolymerization reaction. (D) Effect of PEG4SH concentration on modulus (G') of GeNB (5 wt %) hydrogels. (E) Modulus of various gelatin-based hydrogels, all cross-linked with 5 wt % (GelNB or GelNB-Hep). Mass loss profiles of hydrogels treated with exogenously added (F) type 1 collagenase or (G) hyaluronidase. Hydrogels were fabricated with 5 wt % GelNB cross-linked with either PEG4SH (0.6 wt %) or THA (0.4 wt %) and 2 mM LAP. For heparin-containing hydrogels, 0.1 wt % HepTz was preconjugated to macromer GelNB. All cross-linking was conducted under 2 min of 365 nm light exposure. Significance was determined using a one-way ANOVA with Tukey test to compare significance between each group ($N = 3$ gels per condition, * and *** represent $p <$ 0.05 and 0.001, respectively).

2.10. Statistical Analysis. As specified, a one-way or two-way analysis of variance (ANOVA) with a Tukey's post-hoc test was conducted. Statistical significance was considered at a p value of <0.05. Single, double, triple, and quadruple asterisks were used to represent p values of <0.05, 0.01, 0.001, and 0.0001, respectively. The mean ± SEM was used to represent quantitative results. At least three independent repeats were conducted for each experiment.

3. RESULTS AND DISCUSSION

3.1. Macromer Synthesis and Characterization. The iEDDA click reaction between Tz (on HepTz) and NB (on GelNB) moieties was employed to prepare the GelNB-Hep macromer for iPSC encapsulation and differentiation (Figure 1A–C). The Tz-NB iEDDA click reaction is an efficient method

https://doi.org/10.1021/acs.biomac.2c00585
Biomacromolecules 2022, 23, 4141−4152

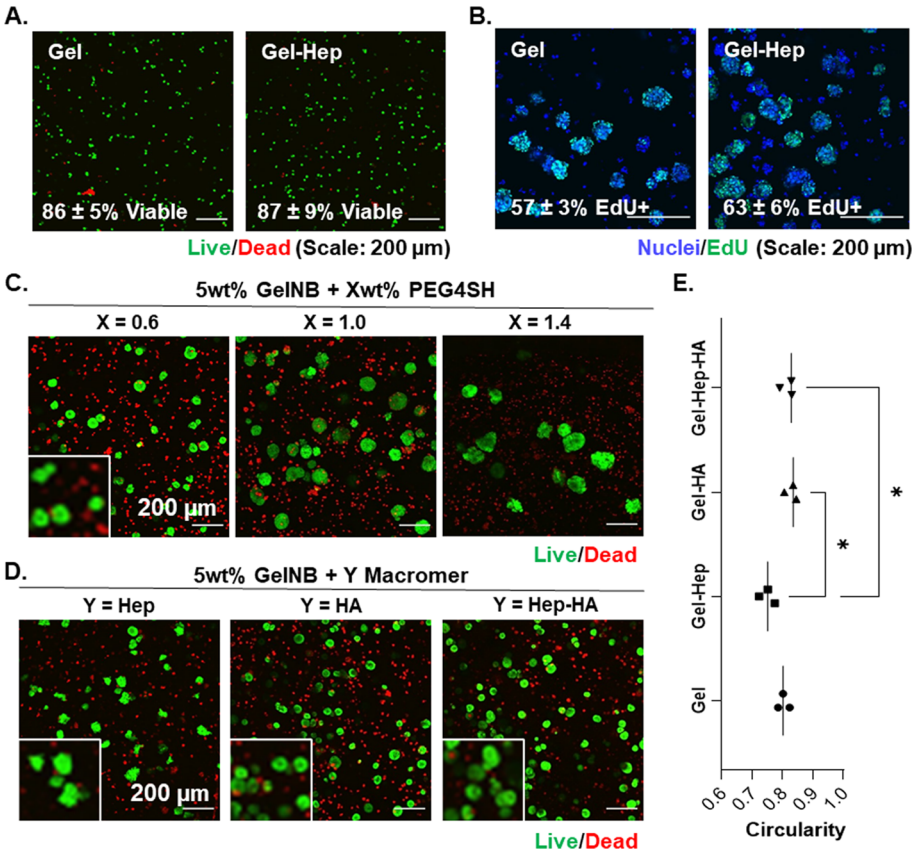

Figure 3. (A) Viability of iPSCs 1 h post-encapsulation in Gel and Gel-Hep hydrogels fabricated with 5 wt % GelNB with or without 0.1 wt % HepTz cross-linked with PEG4SH (0.6 wt %). Percent viability was quantified using ImageJ software. Results are presented as mean ± SD (N = 3). (B) Proliferation of iPSCs in Gel and Gel-Hep hydrogels on D4 post-encapsulation. Percent EdU+ was determined using ImageJ software. Results are presented as mean ± SD (N = 3). (C) Effect of PEG4SH concentration on iPSC aggregate viability D4 post-encapsulation. (D) Viability and (E) circularity of iPSC aggregates in Gel-Hep, Gel-HA, and Gel-Hep-HA hydrogel D4 post-encapsulation. At least three independent regions of interest were imaged (z-stacked image, 10 slices, 10 μm per slice).

commonly used for bioconjugation (e.g., attachment of fluorophores to proteins)[37] and is increasingly employed for fabrication of biomaterials.[38] In this work, standard carbodiimide coupling was first utilized to synthesize HepTz and GelNB, followed by simple mixing of the two macromers for "clicking" heparin to GelNB. Successful clicking/conjugation of HepTz to GelNB was verified via quantification of the Tz characteristic absorbance peak at 523 nm (A_{523nm}).[7] In the presence of GelNB (5 wt %, ~18 mM NB), a steady decrease of A_{523nm} was observed, indicating consumption of Tz (0.5 wt % HepTz, ~0.75 mM initial Tz concentration) (Figure 1D). Near complete Tz consumption was observed after 10 h at 37 °C (Figure 1E). Of note, incubation of HepTz alone over 10 h also led to slight reduction of A_{523nm} (~10%), presumably due to the instability of the Tz moiety at extended incubation times at 37 °C.[39] In all studies, the concentration of the NB moiety on GelNB was used in >100-fold excess to that of the Tz moiety on HepTz. Therefore, given that the iEDDA reaction follows second order rate laws,[40] it is likely that all Tz is consumed well before the ~16 h incubation time prior to gelation. The immobilization of heparin in Gel-Hep hydrogels was confirmed by the intense purple color of the DMMB reagent following extensive rinse to remove unbound reagent (Figure 1F).[41] While heparin is utilized in this study, the Tz-NB reaction could be extended to generate a multitude of other macromer−macromer or ligand−macromer (e.g., RGDS-PEG) combinations.

3.2. Modular Cross-Linking of Gelatin-Based Hydrogels. After confirming heparin conjugation to GelNB through the Tz-NB iEDDA click reaction, thiol-norbornene photopolymerization was used to cross-link the primary hydrogel network with either GelNB (denoted as "Gel") or GelNB-Hep (denoted as "Gel-Hep") macromers. Inert PEG4SH (Figure 2A) and bioactive THA (Figure 2B) were utilized for the thiol-ene cross-linking reaction (Figure 2C). While the Tz-NB iEDDA click reaction could also be used to generate the primary cross-linking network, thiol-norbornene photopolymerization minimizes the working time to preserve the viability of highly sensitive cell types such as iPSCs. In fact, thiol-norbornene photopolymerization has been successfully used to encapsulate iPSCs for their proliferation and differentiation in 3D.[7,42] Without altering the bioactive gelatin macromer content (i.e., 5 wt % GelNB), moduli of the hydrogels were readily tuned by adjusting multi-functional thiol cross-linker (e.g., PEG4SH). For example, increasing the cross-linker PEG4SH concentration from 0.6 to 1.4 wt % led to a G' value of ~1.5 to ~3.5 kPa (Figure 2D).

The use of modular thiol-norbornene photopolymerization also permitted the cross-linking of hydrogels with different compositions but similar moduli (~1.5 kPa. Figure 2E). Similarly, the swelling ratios of these hydrogels were kept relatively unchanged across all conditions, with values of 21 ± 0.9, 20 ± 0.1, 19 ± 0.8, and 18 ± 0.7 for Gel, Gel-Hep, Gel-HA, and Gel-Hep-HA hydrogels, respectively. As these hydrogels

https://doi.org/10.1021/acs.biomac.2c00585
Biomacromolecules 2022, 23, 4141−4152

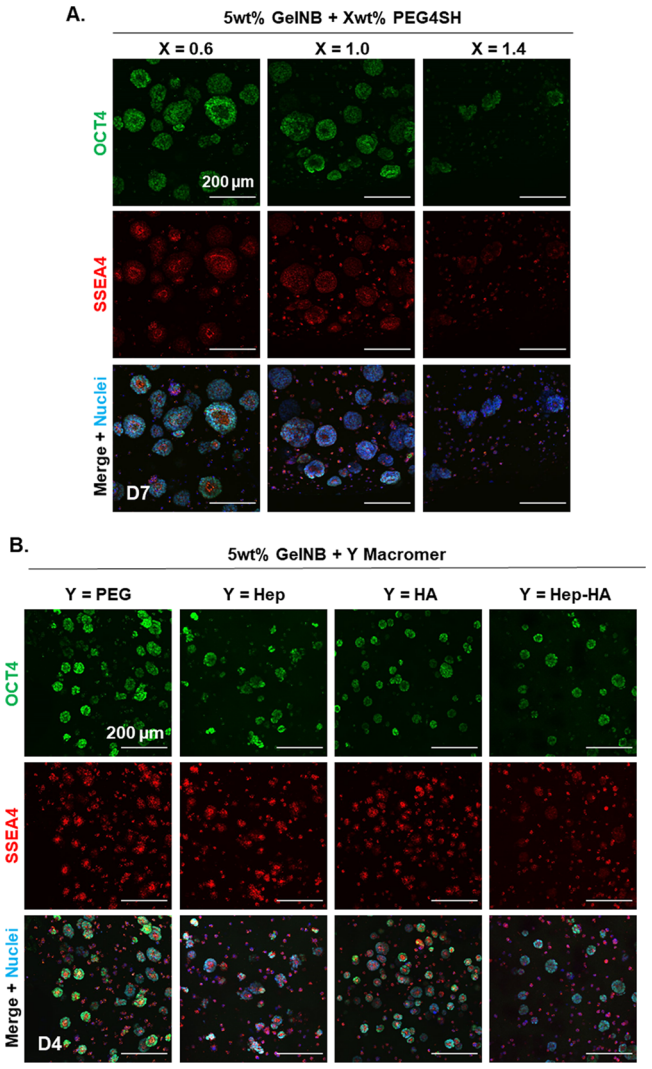

Figure 4. (A) Effect of PEG4SH concentration on pluripotency marker expression OCT4/SSEA4 on D7 post-encapsulation. (B) Pluripotency marker expression in Gel, Gel-Hep, Gel-HA, and Gel-Hep-HA on D4 post-encapsulation. At least three independent regions of interest were imaged (z-stacked image, 10 slices, 10 μm per slice).

were cross-linked by gelatin and in some conditions with HA, collagenase and hyaluronidase were used to evaluate protease-mediated matrix degradation. As expected, all gelatin-based hydrogels treated with type 1 collagenase were completely degraded eventually, albeit with different degradation behaviors. Specifically, the mass of Gel and Gel-Hep hydrogels decreased monotonically immediately following collagenase treatment and were unmeasurable after 1 h of enzyme treatment. On the other hand, the mass of HA-containing hydrogels increased initially, followed by rapid decreases and the gels become unmeasurable after 2 to 2.5 h (Figure 2F). The initial gain in mass of THA-containing hydrogels was attributed to the high water-imbibing ability of HA. Hydrogel mass started to decrease once the sufficient degree of network cleavage occurred. When hydrogels were treated with hyaluronidase, only gels cross-linked with THA showed noticeable degradation (Figure 2G). These data collectively show that the hydrogel biochemical and mechanical properties can be precisely tuned for encapsulation.

3.3. Effect of Hydrogel Properties on iPSC Viability and Pluripotency. To assess the cytocompatibility of thiol-norbornene photocross-linking on hiPSCs, we first examined the effect of the cross-linking/conjugation reactions on the viability of ChiPSC12 cells encapsulated in Gel and Gel-Hep hydrogels cross-linked by PEG4SH. The viability of hiPSCs in the GelNB and GelNB-Hep hydrogels was assessed by live/dead staining 1 h post-encapsulation. As shown in Figure 3A, viability was relatively high following the cross-linking reaction (~86−88% viable cells). While some dead cells were visible by D4 post-encapsulation (Figure 3C,D), the surviving cells were highly proliferative and formed embryoid body-like aggregates (Figure 3B). Specifically, ~60% of the cells were EdU+ during the 24 h treatment starting on D3 post-encapsulation. We further evaluated the metabolic activity of hiPSCs maintained in the 2D culture without treatment (control) or treated with Gel (or Gel-Hep) and monofunctional PEG-SH along with photoinitiator LAP. Monofunctional PEG-SH was used as a surrogate for the thiol-norbornene photo-click reaction with GelNB as it permitted the same thiol-norbornene reaction without producing a cross-linked hydrogel network. No noticeable difference was found in the metabolic activities 3 days post-treatment (Figure S1). In this non-gelling condition, dead cells were easily washed away from the 2D culture and the cells alive exhibited similar metabolic activity. Therefore, we conclude that the dead cells seen after several days of culture in 3D hydrogels were a natural process for hiPSCs, as detached dead cells and debris encapsulated in hydrogels were not readily removed from the 3D hydrogels.

We then fixed the content of GelNB at 5 wt %, while increasing the cross-linker PEG4SH concentration to evaluate cell viability in hydrogels with different stiffness values (Figure 2D). Consistent with a prior work in synthetic PEG-peptide hydrogels, the cross-linking density of the gelatin-based hydrogels affected the viability, size, and morphology of iPSC aggregates (Figure 3C). Specifically, there were considerably fewer but morphologically irregular aggregates formed in the hydrogels cross-linked by 1.4 wt % PEG4SH, the group with the highest cross-linking density. We reasoned that hydrogels with higher cross-linking density would lead to higher matrix stress than the encapsulated cells, leading to higher frequency of cell death. The mechanism leading to irregularities in size and morphology of aggregates in stiffer hydrogels remains unclear. When gelatin-based hydrogels were cross-linked at a relatively low modulus of ~1 kPa, qualitatively, no noticeable difference was found in cell viability or frequency of aggregate formation in the Hep, HA, and Hep-HA conditions (Figure 3D). However, the morphology of aggregates in the Gel-Hep hydrogels were less spherical as determined by quantifying circularity of the aggregates (Figure 3E). Interestingly, iPSC aggregates in the Gel-Hep-HA conditions were significantly more circular than the Gel-Hep hydrogels alone. Heparin has been shown to modulate the canonical Wnt signaling pathway and its downstream effectors of cell motility.[11,43,44] We speculated that the addition of immobilized heparin may be inducing iPSC protrusions due to increased Wnt activation and beta-catenin nuclear stabilization. Additional mechanistic studies are needed to test this hypothesis. The structural compositions of cross-linkers PEG4SH or THA may be leading to the restoration of the spherical clusters observed in the Gel-HA and Gel-Hep-HA hydrogels. The exact mechanism is unclear, and future studies are warranted to elucidate the cause for this phenomenon.

3.4. Growth of iPSCs in Heparinized Gelatin-Based Hydrogels. Given the observed differences with varied hydrogel cross-linking density/compositions on iPSC aggre-

https://doi.org/10.1021/acs.biomac.2c00585
Biomacromolecules 2022, 23, 4141−4152

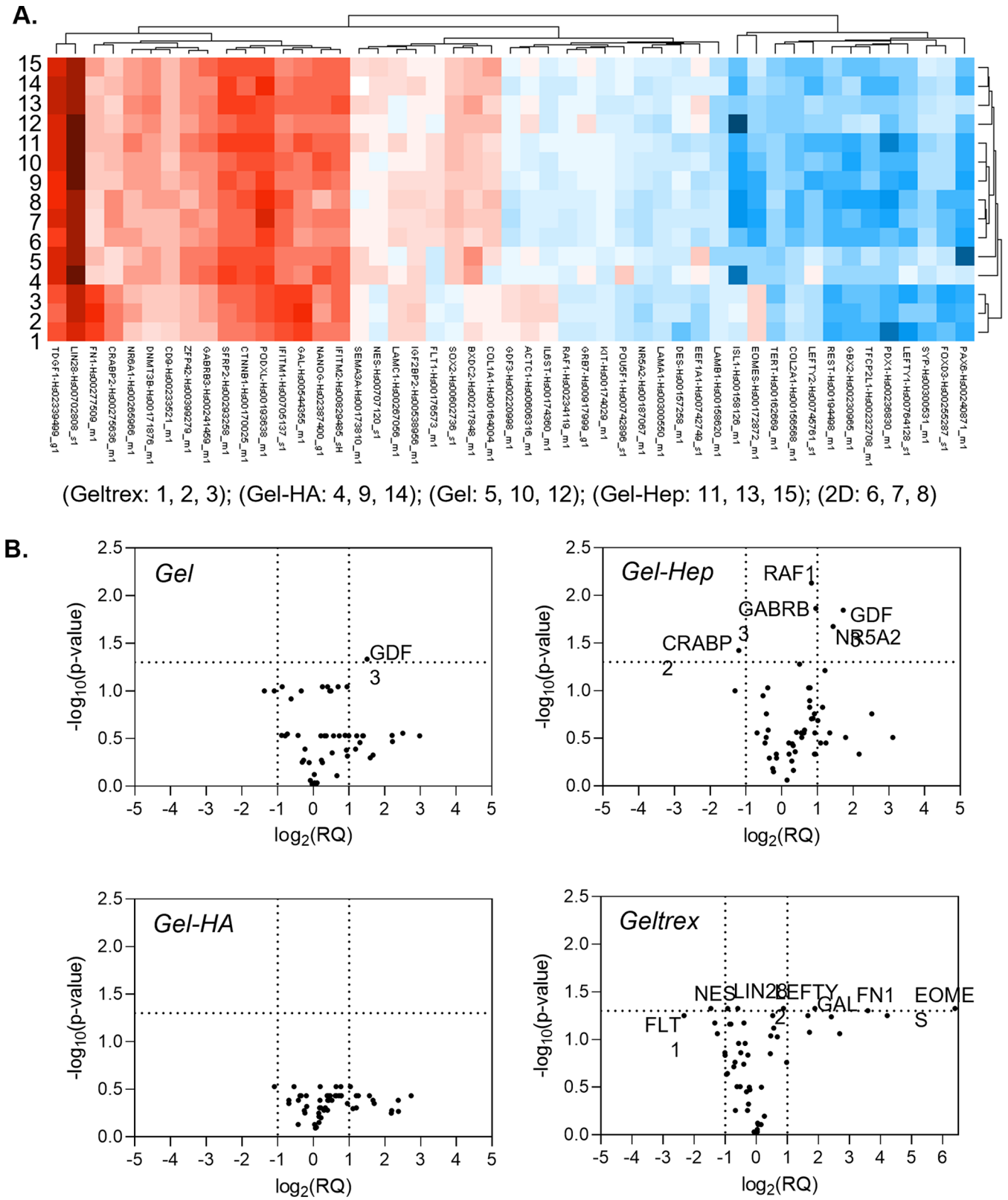

Figure 5. (A) Stem cell-associated gene expression 2D, Geltrex, Gel, Gel-Hep, and Gel-HA hydrogels. Gene expression levels were quantified via RQ analysis with the global normalization group. Each formulation contained three biological replicates. Higher expression is represented by red colors, whereas lower expression is indicated by blue colors. Detailed gene labels are shown in Figure S2. (B) Volcano plots showing differentially expressed genes in each hydrogel condition. Dotted lines represent +/− 2-fold change in expression, and p-value < 0.05.

gates, particularly in the stiffer Gel hydrogels and the Gel-Hep hydrogels of lower stiffness, expression levels of stem cell- and differentiation-associated molecular markers were assessed via immunostaining (Figure 4) and qRT-PCR (Figure 5). Of note, pluripotency of encapsulated iPSCs appeared to be reduced at a higher modulus as shown by diminishing OCT4/SSEA4

https://doi.org/10.1021/acs.biomac.2c00585
Biomacromolecules 2022, 23, 4141−4152

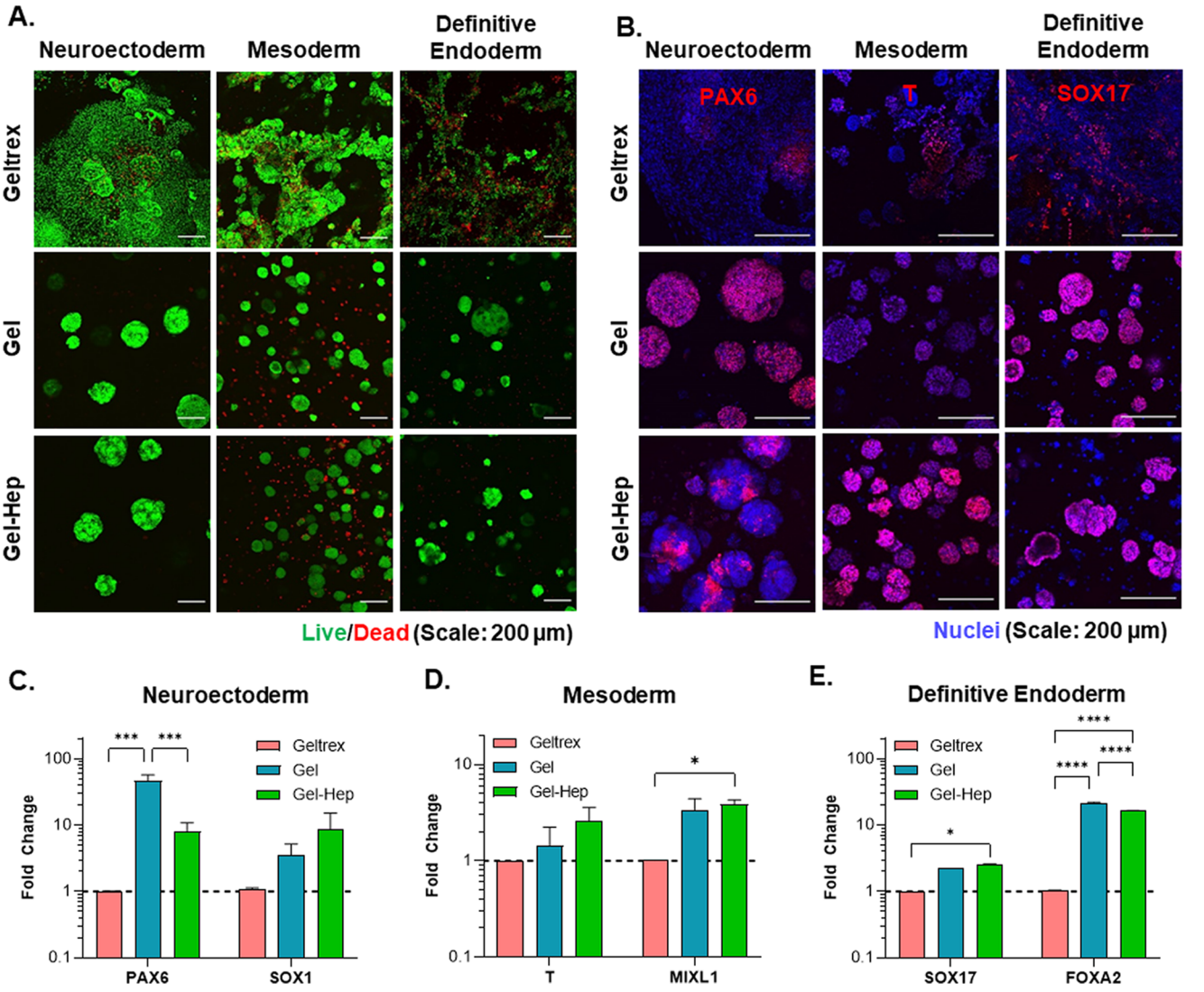

Figure 6. Representative (A) live/dead and (B) immunostaining and imaging of cells after NE, mesoderm, and DE differentiation in the Geltrex, Gel, and Gel-Hep conditions. Characteristic expression of genes unique to neuroectoderm (C), mesoderm (D), and definitive endoderm (E) was performed using qRCR. Gene expression at the mRNA levels were normalized to housekeeping gene 18S. Significance was determined using a two-way ANOVA with Tukey test to compare significance between each group (N = 3 gels per condition, *, ***, and **** represent $p < 0.05$, 0.001, and 0.0001, respectively).

staining (Figure 4A). In contrast, OCT4/SSEA4 expression appears to be largely maintained in the Gel, Gel-Hep, and Gel-HA hydrogels after 4 days of culture (Figure 4B), suggesting that HepTz functionalization and THA cross-linking did not significantly affect pluripotency in the 3D culture.

We further analyzed the gene expression patterns of iPSCs grown in the multicomponent hydrogels with cells grown in Geltrex and the conventional 2D cell culture plate as 3D and 2D controls, respectively (Figure 5). Hierarchical clustering analysis revealed broad differences in stem cell marker expression in Geltrex-encapsulated iPSCs relative to the other three conditions (Figure 5A, Figure S2). To our surprise, clustering analysis identified high similarity of gene expression between iPSCs grown in 3D gelatin-based hydrogels and in 2D control samples. This suggests that both the vitronectin-coated 2D cell culture strategy and the gelatin-based multifunctional hydrogels provide sufficient E-cadherin-mediated cell−cell interactions and integrin-mediated cell-ECM to maintain the pluripotency and self-renewal of the iPSCs over the 4 day culture time.[45]

Results of statistical analyses were represented in the volcano plots to identify significantly upregulated and downregulated genes (Figure 5B). In particular, aggregates in the Gel and Gel-Hep hydrogels have elevated expression of growth differentiation factor 3 (GDF3), a member of the TGFβ family and associated with stem cell pluripotency.[46,47] Interestingly, unlike Gel and Gel-Hep, addition of HA did not yield significant upregulation of GDF3. Of the multicomponent hydrogels, Gel-Hep also led to significant elevation of nuclear receptor subfamily 5 group a member 2 (NR5A2), which has been shown to regulate stem cell pluripotency.[48] Downregulated genes in Gel-Hep hydrogels included cellular retinoic acid binding protein 2 (CRABP2). Aside from these few genes, no significant changes in cell pluripotency genes (e.g., OCT4, SOX2, NANOG) were detected; confirming that the Gel, Gel-Hep, and Gel-HA hydrogels did not negatively affect iPSC pluripotency. Consistent with other studies using basement membrane extracts for iPSC encapsulation,[49] Geltrex led to significant upregulation of differentiation associated genes

https://doi.org/10.1021/acs.biomac.2c00585
Biomacromolecules 2022, 23, 4141−4152

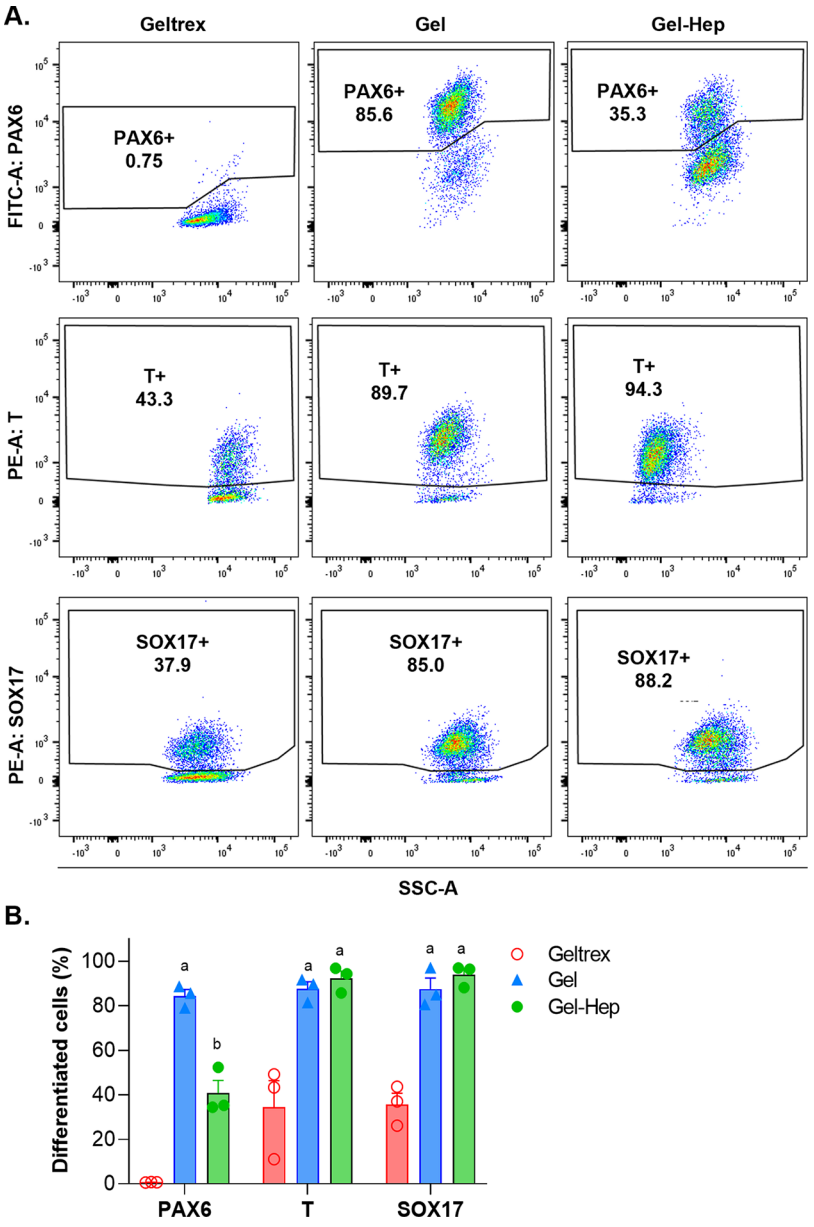

Figure 7. (A) Representative flow cytometry results after NE, mesoderm, and DE differentiation in Geltrex, Gel, and Gel-Hep conditions. (B) Numerical summary of flow cytometry results. Significance was determined using a two-way ANOVA with Tukey test to compare significance between each group ($N = 3$ gels per condition, "a" represents $p < 0.0001$ relative to Geltrex, "b" represents $p < 0.001$ relative to Geltrex, and "c" represents $p < 0.001$ relative to Gel.

fibronectin 1 (FN1) and eomesodermin (EOMES). However, pluripotency-associated genes were not significantly down-regulated in Geltrex, suggesting the presence of undifferentiated iPSCs. In contrast, the panel results combined with the immunostaining results suggest that the multicomponent gelatin-based hydrogels may be suitable for culturing iPSC aggregates in 3D.

3.5. Trilineage Differentiation of iPSCs in Heparinized Gelatin-Based Hydrogels. Trilineage differentiation was utilized to assess the differentiation potential of gelatin-encapsulated iPSCs toward the ectoderm (including non-neuroectoderm (NNE) and neuroectoderm (NE)), mesoderm, and definitive endoderm (DE) (Figure S3, Figures 6 and 7). Results were compared against differentiation of iPSCs in 3D Geltrex-based hydrogels. Of note, we did not pursue differentiation of iPSCs in the presence of HA given our observations regarding the similarities in cell viability and stem cell marker expression in Figures 3−5. Interestingly, after differentiation, significantly more cell deaths were observed in the Geltrex hydrogels but less in the surviving aggregates in the Gel and Gel-Hep hydrogels (Figure 6A). Further, differentiated iPSCs in Geltrex hydrogels exhibited a higher degree of spreading in all three germ layers relative to the Gel and Gel-Hep conditions. Interestingly, lobular structures were apparent in the NE-differentiated iPSC aggregates in the Gel and Gel-Hep conditions.

In addition to the viability and morphology, distinct differentiation outcome was observed between the Geltrex, Gel, and Gel-Hep hydrogels. Of note, NNE differentiation was conducted with minimal efficiency for all hydrogel-based conditions as indicated by a lack of expression of transcription factor AP-2α (TFAP2α) (Figure S3). Unsuccessful NNE

https://doi.org/10.1021/acs.biomac.2c00585
Biomacromolecules 2022, 23, 4141−4152

differentiation might be due to the general differences in protocols. In prior studies, NNE differentiation was conducted with embryoid bodies in a suspension culture as opposed to single cell encapsulation in this study.[36] With respect to NE differentiation, considerable differences in paired box protein Pax-6 (PAX6) expression were observed across all three conditions. The highest degree of PAX6+ NE cells was present in the Gel condition, compared with significantly fewer numbers of PAX6+ cells in the Gel-Hep and Geltrex conditions (Figures 6B and 7). This was accompanied by high PAX6 and SOX1 gene expression relative to the Geltrex control (Figure 6C). Interestingly, we observed slightly elevated SOX1 expression as well as significant differences in aggregate morphology comparing the Gel and Gel-Hep conditions (Figure S4). We also observed rosette structures in the Gel-Hep hydrogels, which were not as readily apparent in the Gel hydrogels (Figure S4). The characteristic rosette structures accompanied by PAX6-positive neuroepithelium marker in the Gel-Hep hydrogels may be an area of future work. Regardless, we show that the Gel-based hydrogels exhibit efficient NE differentiation and may be useful in establishing models of neural development and disease.

Prior studies have shown the effect of soluble heparin on mesoderm lineage commitment.[12] Therefore, the effect of immobilized heparin within the gelatin-based hydrogels on mesoderm differentiation was also assessed and compared against Gel hydrogels. Immunostaining results revealed a percentage of cells in Gel hydrogels stained positive for Brachyury (T), but the fluorescence intensity was considerably low (Figure 6B). Very limited T-positive cells were detected in the Geltrex condition; however, over 90% of cells in the Gel hydrogels were positive for T (Figures 6B and 7). Interestingly, while the expression of T was only elevated ∼1.44-fold with no significant difference in Geltrex and Gel gels, Mix1 homeobox (MIXL1) was elevated ∼3.4 in the Gel hydrogels (Figure 6D). The reason for the differences in the T gene expression and immunostaining result is unclear, but it is speculated that the gene expression levels may explain the relatively low fluorescence intensity in the Gel condition. Flow cytometry results confirmed the significant increase in T-positive cells in both the Gel and Gel-Hep hydrogels relative to the Geltrex control (Figure 7). It is hypothesized that heparin may be acting on the Wnt signaling pathway along with the soluble GSK3β inhibitor, CHIR99021, to drive early mesoderm commitment; however, further investigation is required.

In DE differentiation, fewer SRY-BOX transcription factor 17 (SOX17)-positive cells were present in Geltrex relative to Gel and Gel-Hep (Figure 6B) after DE differentiation. Flow cytometry analyses confirmed the immunostaining results with significantly higher degree of differentiated cells (Figure 7). Consistent with the immunostaining results, both SOX17 and Forkhead Box A2 (FOXA2) expressions were elevated in the Gel and Gel-Hep hydrogels (Figure 6E). While mesoderm differentiation was affected by the presence of heparin, the Gel-Hep hydrogels did not significantly improve definitive endoderm differentiation. Like mesoderm differentiation, definitive endoderm differentiation requires Wnt activation through small molecule treatment or the addition of exogenous recombinant Wnt and also requires modulation of the Activin/NODAL pathways.[50] Given that heparin has been shown to have affinity for Activin A,[51] which is commonly used to induce definitive endoderm differentiation, it was expected that the hydrogels may influence endoderm lineage commitment in 3D; however, the gelatin-based hydrogels alone were sufficient for DE differentiation.

4. CONCLUSIONS

In this work, we integrated the tetrazine-norbornene iEDDA click reaction and thiol-norbornene photopolymerization to generate bioactive multicomponent hydrogels for culture and differentiation of hiPSCs. hiPSCs were encapsulated in gelatin-based thiol-norbornene hydrogels with high viability, and the encapsulated cells formed proliferative embryoid body-like clusters. We found that engineered GelNB hydrogels were superior to naturally derived Geltrx in supporting differentiation of NE, mesoderm, and DE lineages but not for NNE commitment. We further identified that the immobilization of heparin in the gelatin-based hydrogels led to slight reduction of PAX6 expression in NE differentiation but promoted formation of the neural rosette structure. Our results also suggest that the multicomponent gelatin-based hydrogels may be particularly suited for DE differentiation. Future work will explore the use of these hydrogels for neural and pancreatic organoid generation.

■ ASSOCIATED CONTENT

Supporting Information

The Supporting Information is available free of charge at https://pubs.acs.org/doi/10.1021/acs.biomac.2c00585.

(Table S1) Formulations used for hydrogel fabrication; (Table S2) list of primers used for real-time PCR; (Figure S1) metabolic activity 1 h and 72 h post-treatment; (Figure S2) Detailed labels of stem cell-associated gene expression 2D, Geltrex, Gel, Gel-Hep, and Gel-HA hydrogels. Gene expression levels were quantified via RQ analysis with global normalization. group. (Figure S3) live/dead and immunostaining images of encapsulated cells after nonneural ectoderm differentiation in Geltrex, Gel, and Gel-Hep hydrogels; and (Figure S4) F-actin and nuclei staining of NE-differentiated aggregates including an equatorial slice and Z-stacked image revealing rosette structure formation (PDF)

■ AUTHOR INFORMATION

Corresponding Author

Chien-Chi Lin − *Weldon School of Biomedical Engineering, Purdue University, West Lafayette, Indiana 47907, United States; Department of Biomedical Engineering, Purdue School of Engineering & Technology, Indiana University-Purdue University Indianapolis, Indianapolis, Indiana 46202, United States;* orcid.org/0000-0002-4175-8796; Phone: (317) 274-0760; Email: lincc@iupui.edu

Authors

Matthew R. Arkenberg − *Weldon School of Biomedical Engineering, Purdue University, West Lafayette, Indiana 47907, United States*

Karl Koehler − *Departments of Otolaryngology and Plastic and Oral Surgery, F.M. Kirby Neurobiology Center, Boston Children's Hospital/Harvard Medical School, Boston, Massachusetts 02115, United States*

Complete contact information is available at: https://pubs.acs.org/10.1021/acs.biomac.2c00585

Notes

The authors declare no competing financial interest.

https://doi.org/10.1021/acs.biomac.2c00585
Biomacromolecules 2022, 23, 4141−4152

■ ACKNOWLEDGMENTS

The authors thank the members of the Indiana University Melvin and Bren Simon Cancer Center Flow Cytometry Resource Facility for their outstanding technical support. The Indiana University Melvin and Bren Simon Comprehensive Cancer Center Flow Cytometry Resource Facility is funded in part by NIH, National Cancer Institute (NCI) grant P30 CA082709, and National Institute of Diabetes and Digestive and Kidney Diseases (NIDDK) grant U54 DK106846. The FCRF is supported in part by NIH instrumentation grant 1S10D012270. The authors would also like to thank Dr. Eri Hashino, Indiana University School of Medicine, for providing materials for non-neural ectoderm differentiation. The authors thank the following funding sources: National Institutes of Health (R01CA227737 and R01DK127436 to C.C.L.; R01DC017461 to K.R.K.), National Science Foundation (CAREER Award DMR1452390 to C.C.L.; Graduate Research Fellowship Program, to M.R.A.), and Thomas J. Linnemeier Guidant Foundation Endowment (to C.C.L.).

■ REFERENCES

(1) Miranda, C. C.; Fernandes, T. G.; Diogo, M. M.; Cabral, J. M. S. Human Pluripotent Stem Cells: Applications and Challenges for Regenerative Medicine and Disease Modeling. *Adv. Biochem. Eng./Biotechnol.* **2020**, *171*, 189−224.

(2) Pennings, S.; Liu, K. J.; Qian, H. The stem cell niche: interactions between stem cells and their environment. *Stem Cells Int.* **2018**, *2018*, 4879379.

(3) Blondel, D.; Lutolf, M. P. Bioinspired hydrogels for 3D organoid culture. *Chimia* **2019**, *73*, 81−85.

(4) Cruz-Acuña, R.; Quirós, M.; Farkas, A. E.; Dedhia, P. H.; Huang, S.; Siuda, D.; García-Hernández, V.; Miller, A. J.; Spence, J. R.; Nusrat, A.; García, A. J. Synthetic hydrogels for human intestinal organoid generation and colonic wound repair. *Nat. Cell Biol.* **2017**, *19*, 1326−1335.

(5) Ekerdt, B. L.; Fuentes, C. M.; Lei, Y.; Adil, M. M.; Ramasubramanian, A.; Segalman, R. A.; Schaffer, D. V. Thermoreversible Hyaluronic Acid-PNIPAAm Hydrogel Systems for 3D Stem Cell Culture. *Adv. Healthcare Mater.* **2018**, *7*, No. e1800225.

(6) Lei, Y.; Schaffer, D. V. A fully defined and scalable 3D culture system for human pluripotent stem cell expansion and differentiation. *Proc. Natl. Acad. Sci. U. S. A.* **2013**, *110*, E5039−E5048.

(7) Arkenberg, M. R.; Dimmitt, N. H.; Johnson, H. C.; Koehler, K. R.; Lin, C. C. Dynamic Click Hydrogels for Xeno-Free Culture of Induced Pluripotent Stem Cells. *Adv. Biosyst.* **2020**, *4*, No. e2000129.

(8) Richardson, T.; Barner, S.; Candiello, J.; Kumta, P. N.; Banerjee, I. Capsule stiffness regulates the efficiency of pancreatic differentiation of human embryonic stem cells. *Acta Biomater.* **2016**, *35*, 153−165.

(9) Siltanen, C.; Yaghoobi, M.; Haque, A.; You, J.; Lowen, J.; Soleimani, M.; Revzin, A. Microfluidic fabrication of bioactive microgels for rapid formation and enhanced differentiation of stem cell spheroids. *Acta Biomater.* **2016**, *34*, 125−132.

(10) Nazari, B.; Kazemi, M.; Kamyab, A.; Nazari, B.; Ebrahimi-Barough, S.; Hadjighassem, M.; Norouzi-Javidan, A.; Ai, A.; Ahmadi, A.; Ai, J. Fibrin hydrogel as a scaffold for differentiation of induced pluripotent stem cells into oligodendrocytes. *J. Biomed. Mater. Res., B* **2020**, *108*, 192−200.

(11) Colombres, M.; Henriquez, J. P.; Reig, G. F.; Scheu, J.; Calderon, R.; Alvarez, A.; Brandan, E.; Inestrosa, N. C. Heparin activates Wnt signaling for neuronal morphogenesis. *J. Cell. Physiol.* **2008**, *216*, 805−815.

(12) Lin, Y.; Linask, K. L.; Mallon, B.; Johnson, K.; Klein, M.; Beers, J.; Xie, W.; Du, Y.; Liu, C.; Lai, Y. Heparin promotes cardiac differentiation of human pluripotent stem cells in chemically defined albumin-free medium, enabling consistent manufacture of cardiomyocytes. *Stem Cells Transl. Med.* **2017**, *6*, 527−538.

(13) Gerecht, S.; Burdick, J. A.; Ferreira, L. S.; Townsend, S. A.; Langer, R.; Vunjak-Novakovic, G. Hyaluronic acid hydrogel for controlled self-renewal and differentiation of human embryonic stem cells. *Proc. Natl. Acad. Sci. U. S. A.* **2007**, *104*, 11298−11303.

(14) Miura, T.; Yuasa, N.; Ota, H.; Habu, M.; Kawano, M.; Nakayama, F.; Nishihara, S. Highly sulfated hyaluronic acid maintains human induced pluripotent stem cells under feeder-free and bFGF-free conditions. *Biochem. Biophys. Res. Commun.* **2019**, *518*, 506−512.

(15) Bejoy, J.; Wang, Z.; Bijonowski, B.; Yang, M.; Ma, T.; Sang, Q. X.; Li, Y. Differential Effects of Heparin and Hyaluronic Acid on Neural Patterning of Human Induced Pluripotent Stem Cells. *ACS Biomater. Sci. Eng.* **2018**, *4*, 4354−4366.

(16) Furue, M. K.; Na, J.; Jackson, J. P.; Okamoto, T.; Jones, M.; Baker, D.; Hata, R.; Moore, H. D.; Sato, J. D.; Andrews, P. W. Heparin promotes the growth of human embryonic stem cells in a defined serum-free medium. *Proc. Natl. Acad. Sci. U. S. A.* **2008**, *105*, 13409−13414.

(17) Lyon, M.; Rushton, G.; Gallagher, J. T. The interaction of the transforming growth factor-betas with heparin/heparan sulfate is isoform-specific. *J. Biol. Chem.* **1997**, *272*, 18000−18006.

(18) Vemuri, S.; Beylin, I.; Sluzky, V.; Stratton, P.; Eberlein, G.; Wang, Y. J. The stability of bFGF against thermal denaturation. *J. Pharm. Pharmacol.* **1994**, *46*, 481−486.

(19) Chen, G.; Gulbranson, D. R.; Hou, Z.; Bolin, J. M.; Ruotti, V.; Probasco, M. D.; Smuga-Otto, K.; Howden, S. E.; Diol, N. R.; Propson, N. E.; et al. Chemically defined conditions for human iPSC derivation and culture. *Nat. Methods* **2011**, *8*, 424−429.

(20) Greene, T.; Lin, C.-C. Modular cross-linking of gelatin-based thiol−norbornene hydrogels for in vitro 3D culture of hepatocellular carcinoma cells. *ACS Biomater. Sci. Eng.* **2015**, *1*, 1314−1323.

(21) Bragg, J. C.; Kweon, H.; Jo, Y.; Lee, K. G.; Lin, C.-C. In situ formation of silk-gelatin hybrid hydrogels for affinity-based growth factor sequestration and release. *RSC Adv.* **2016**, *6*, 114353−114360.

(22) Schirmer, L.; Atallah, P.; Werner, C.; Freudenberg, U. StarPEG-Heparin Hydrogels to Protect and Sustainably Deliver IL-4. *Adv. Healthcare Mater.* **2016**, *5*, 3157−3164.

(23) Tae, G.; Kim, Y. J.; Choi, W. I.; Kim, M.; Stayton, P. S.; Hoffman, A. S. Formation of a novel heparin-based hydrogel in the presence of heparin-binding biomolecules. *Biomacromolecules* **2007**, *8*, 1979−1986.

(24) Peuler, K.; Dimmitt, N.; Lin, C. C. Clickable modular polysaccharide nanoparticles for selective cell-targeting. *Carbohydr. Polym.* **2020**, *234*, No. 115901.

(25) Brown, G. C.; Lim, K. S.; Farrugia, B. L.; Hooper, G. J.; Woodfield, T. B. Covalent incorporation of heparin improves chondrogenesis in photocurable gelatin-methacryloyl hydrogels. *Macromol. Biosci.* **2017**, *17*, 1700158.

(26) Toole, B. P. Hyaluronan in morphogenesis. *Semin. Cell Dev. Biol.* **2001**, *12*, 79−87.

(27) Toole, B. P. Hyaluronan: from extracellular glue to pericellular cue. *Nat. Rev. Cancer* **2004**, *4*, 528−539.

(28) Li, Y.; Lin, C.; Wang, L.; Liu, Y.; Mu, X.; Ma, Y.; Li, L. Maintenance of human embryonic stem cells on gelatin. *Chin. Sci. Bull.* **2009**, *54*, 4214−4220.

(29) Kim, D.; Cha, B. H.; Ahn, J.; Arai, Y.; Choi, B.; Lee, S. H. Physicochemical Properties in 3D Hydrogel Modulate Cellular Reprogramming into Induced Pluripotent Stem Cells. *Adv. Funct. Mater.* **2021**, *31*, 2007041.

(30) Jung, J.-H.; Kim, B. S.A novel culture model for human pluripotent stem cell propagation on gelatin in placenta-conditioned media. *J. Visualized Exp.***2015**, (*102*), DOI: 10.3791/53204.

(31) Shih, H.; Greene, T.; Korc, M.; Lin, C. C. Modular and Adaptable Tumor Niche Prepared from Visible Light Initiated Thiol-Norbornene Photopolymerization. *Biomacromolecules* **2016**, *17*, 3872−3882.

(32) Koshy, S. T.; Desai, R. M.; Joly, P.; Li, J.; Bagrodia, R. K.; Lewin, S. A.; Joshi, N. S.; Mooney, D. J. Click-Crosslinked Injectable Gelatin Hydrogels. *Adv. Healthcare Mater.* **2016**, *5*, 541−547.

(33) Alge, D. L.; Azagarsamy, M. A.; Donohue, D. F.; Anseth, K. S. Synthetically tractable click hydrogels for three-dimensional cell culture

formed using tetrazine-norbornene chemistry. *Biomacromolecules* **2013**, *14*, 949−953.
(34) Mũnoz, Z.; Shih, H.; Lin, C.-C. Gelatin hydrogels formed by orthogonal thiol−norbornene photochemistry for cell encapsulation. *Biomater. Sci.* **2014**, *2*, 1063−1072.
(35) Crosby, C. O.; Valliappan, D.; Shu, D.; Kumar, S.; Tu, C.; Deng, W.; Parekh, S. H.; Zoldan, J. Quantifying the Vasculogenic Potential of Induced Pluripotent Stem Cell-Derived Endothelial Progenitors in Collagen Hydrogels. *Tissue Eng.. A* **2019**, *25*, 746−758.
(36) Nie, J.; Hashino, E. Generation of inner ear organoids from human pluripotent stem cells. *Methods Cell Biol.* **2020**, *159*, 303−321.
(37) Kim, E.; Koo, H. Biomedical applications of copper-free click chemistry: in vitro, in vivo, and ex vivo. *Chem. Sci.* **2019**, *10*, 7835−7851.
(38) Arkenberg, M. R.; Nguyen, H. D.; Lin, C.-C. Recent advances in bio-orthogonal and dynamic crosslinking of biomimetic hydrogels. *J. Mater. Chem. B* **2020**, *8*, 7835−7855.
(39) Karver, M. R.; Weissleder, R.; Hilderbrand, S. A. Synthesis and evaluation of a series of 1, 2, 4, 5-tetrazines for bioorthogonal conjugation. *Bioconjugate Chem.* **2011**, *22*, 2263−2270.
(40) Knall, A.-C.; Hollauf, M.; Slugovc, C. Kinetic studies of inverse electron demand Diels−Alder reactions (iEDDA) of norbornenes and 3, 6-dipyridin-2-yl-1, 2, 4, 5-tetrazine. *Tetrahedron Lett.* **2014**, *55*, 4763−4766.
(41) Templeton, D. M. The basis and applicability of the dimethylmethylene blue binding assay for sulfated glycosaminoglycans. *Connect. Tissue Res.* **1988**, *17*, 23−32.
(42) Ovadia, E. M.; Colby, D. W.; Kloxin, A. M. Designing well-defined photopolymerized synthetic matrices for three-dimensional culture and differentiation of induced pluripotent stem cells. *Biomaterials Sci.* **2018**, *6*, 1358−1370.
(43) Berendsen, A. D.; Fisher, L. W.; Kilts, T. M.; Owens, R. T.; Robey, P. G.; Gutkind, J. S.; Young, M. F. Modulation of canonical Wnt signaling by the extracellular matrix component biglycan. *Proc. Natl. Acad. Sci. U. S. A.* **2011**, *108*, 17022−17027.
(44) Sineva, G. S.; Pospelov, V. A. β-Catenin in pluripotency: adhering to self-renewal or Wnting to differentiate? *Int. Rev. Cell Mol. Biol.* **2014**, *312*, 53−78.
(45) Li, L.; Bennett, S. A.; Wang, L. Role of E-cadherin and other cell adhesion molecules in survival and differentiation of human pluripotent stem cells. *Cell Adhes. Migr.* **2012**, *6*, 59−73.
(46) Xiong, K.; Zhou, Y.; Hyttel, P.; Bolund, L.; Freude, K. K.; Luo, Y. Generation of induced pluripotent stem cells (iPSCs) stably expressing CRISPR-based synergistic activation mediator (SAM). *Stem Cell Res.* **2016**, *17*, 665−669.
(47) Chng, Z.; Vallier, L.; Pedersen, R. Activin/nodal signaling and pluripotency. *Vitam. Horm.* **2011**, *85*, 39−58.
(48) Byers, C.; Spruce, C.; Fortin, H. J.; Hartig, E. I.; Czechanski, A.; Munger, S. C.; Reinholdt, L. G.; Skelly, D. A.; Baker, C. L. Genetic control of the pluripotency epigenome determines differentiation bias in mouse embryonic stem cells. *EMBO J.* **2022**, *41*, No. e109445.
(49) Aisenbrey, E. A.; Murphy, W. L. Synthetic alternatives to Matrigel. *Nat. Rev. Mater.* **2020**, *5*, 539−551.
(50) Dziedzicka, D.; Tewary, M.; Keller, A.; Tilleman, L.; Prochazka, L.; Östblom, J.; Couvreu De Deckersberg, E.; Markouli, C.; Franck, S.; Van Nieuwerburgh, F. Endogenous suppression of WNT signalling in human embryonic stem cells leads to low differentiation propensity towards definitive endoderm. *Sci. Rep.* **2021**, *11*, 1−14.
(51) Li, S.; Shimono, C.; Norioka, N.; Nakano, I.; Okubo, T.; Yagi, Y.; Hayashi, M.; Sato, Y.; Fujisaki, H.; Hattori, S.; Sugiura, N.; Kimata, K.; Sekiguchi, K. Activin A binds to perlecan through its pro-region that has heparin/heparan sulfate binding activity. *J. Biol. Chem.* **2010**, *285*, 36645−36655.

https://doi.org/10.1021/acs.biomac.2c00585
Biomacromolecules 2022, 23, 4141−4152